



Extent, accuracy and repeatability of bare sand and vegetation cover in dunes mapped from aerial imagery is highly variable

Thomas A.G. Smyth^{a,b,1,*}, Ryan Wilson^{a,2}, Paul Rooney^c, Katherine L. Yates^{d,3}

^a Department of Biological and Geographical Sciences, School of Applied Sciences, University of Huddersfield, Huddersfield HD1 3DH, UK

^b Beach and Dune Systems (BEADS) Laboratory, College of Science and Engineering, Flinders University, Adelaide, South Australia, Australia

^c Department of Geography and Environmental Science, Liverpool Hope University, Liverpool, UK

^d School of Science, Engineering and Environment, University of Salford, Manchester, UK

ARTICLE INFO

Keywords:

Coastal dunes
Dune Mobility
Bare Sand
Vegetation Change
Remote Sensing
Image Classification

ABSTRACT

Vegetation cover on coastal sand dunes has been increasing worldwide since at least the 1940s. Analysis of aerial and satellite imagery has been the principal source used to measure this change, however no studies have systematically evaluated the accuracy of remotely sensed estimates. Using established land cover classification methods and in-situ field measurements, we show that both the extent and accuracy of remotely sensed areas of bare sand and vegetation in dunes varies with image resolution and classification method. We found that supervised methods of classification (semi-automatic), whilst mapping a greater extent of bare sand and being more accurate than manual digitisation, had poor repeatability, exhibiting a relatively large range of bare sand and vegetation extent between classifications replicated under the same conditions. In contrast, areas of bare sand and vegetation classified by manual digitisation had high repeatability but a relatively low percentage of observed agreement with data collected in the field. For all classification methods, observed agreement with field data generally increased with image resolution. Our results demonstrate that users of land classification data in dunes should be cautious when interpreting trends of bare sand and vegetation cover due to substantial repeatability error in supervised classification methods, and relatively poor observed agreement with field data of manual classification. We recommend that analysis of bare sand and vegetation cover in dunes should be based on multiple replicates using supervised classification, employing the highest resolution imagery available and that all results presented should also include the range measured by multiple replicates.

Introduction

Aerial photographs and satellite imagery are an important source of information for studies of dune activity in both coastal and inland environments (Table 1). Changes in vegetation and therefore changes in sand dune mobility are most often associated with variations in climate (Pye et al., 2014; Hugenholtz and Wolfe, 2005; Jackson and Cooper, 2011) but also decreased grazing (Levin and Ben-Dor, 2004; Provoost et al., 2011; Pye et al., 2014), changes in land use (Levin and Ben-Dor, 2004; Pye et al., 2014; Moulton et al., 2019; Gao et al., 2020), nutrient enrichment (van Boxel et al., 1997; Pye et al., 2014) and the stabilising role of invasive plant species (Hilton et al., 2005; Provoost et al., 2011; Pickart, 2021). Measurements of coastal dunes around the world have

indicated an overall trend of increased vegetation cover since the 1950s (Hilton, 2006; Pye et al., 2014; Delgado-Fernandez et al., 2019; Jackson et al., 2019; Gao et al., 2020). Increasing vegetation cover resulting in decreased geomorphological dynamism (disturbance) may reduce the biodiversity in dune landscapes habitats (Kutiel, 2001; Pye et al., 2014; Provoost et al., 2011) and decrease the adaptive capacity of the coast to adjust to accelerating sea-level rise (Arens et al., 2020). However, there is also evidence that vegetation growth in foredunes increases their resistance to wave swash allowing coastal sand dunes to provide sustained coastal protection under sustained wave attack (Feagin et al., 2019; De Battisti and Griffin, 2020).

The quantification of changes in bare sand and vegetation has predominantly been performed by the analysis of vertical aerial

* Corresponding author.

¹ 0000-0002-1740-762X.

² 0000-0001-9063-8021.

³ 0000-0001-8429-2941.

photography and satellite imagery both in coastal and continental dunes (Table 1). Studies have used both red, green, blue (RGB) and black and white images as well as multispectral data, from which spectral indices such as normalised difference vegetation index (NDVI) can be derived. The mapping process of this imagery is usually undertaken using three different classification methods, image classification, pixel brightness thresholding, and manual classification (Table 1).

Supervised image classification groups pixels with common spectral characteristics to form a thematic map. The approach (also known as interactive supervised classification and semi-automatic classification) is distinct from unsupervised classification in that a user selects a training set of pixels that are representative of specific land cover categories. Generally, accuracy increases with the number of training samples and identification of all classes within the study area (i.e. water) even if they are not of interest (Foody, 2002; Foody et al., 2006). A similar, but less automated approach, is to classify areas of sand by pixel brightness i.e. the darker the pixel, the more vegetation present (Kutiel

et al., 2004). This method involves adjusting the threshold pixel value to give the best representation of bare sand depending on the brightness of the original photographs (Pye et al., 2014). Manual classification necessitates that an analyst manually delineates (digitises) the boundary of each bare sand patch. Regardless of mapping methods, this process of quantification of bare sand extent is typically performed within a geographical information system.

Studies using these classification methods have undertaken a range of measures to increase the accuracy of remotely sensed bare sand and vegetation. These measures include: radiometric correction/calibration, whereby grey levels are normalised between images (Hugenholtz and Wolfe, 2005; Wolfe et al., 2007); independent reviewing of manual delineation by multiple users (Delgado-Fernandez et al., 2019); the use of a specified number of training pixels for supervised image classification (Hugenholtz and Wolfe, 2005); removal of artificial surfaces and bright areas other than sand (Kutiel et al., 2004; Pye et al., 2014); and the manual correction of improperly classified data (Levin, 2011).

Table 1
Previous studies that have mapped changes in vegetation or bare sand cover in dunes.

Author	Environment	Sensor	Pixel Size	Classification Method	Classifications reported
Wolfe et al., 1995	Continental	Vertical aerial photography	Unspecified	Manual Digitisation	(1) Active dune
Curr et al. 2000	Coastal	Vertical aerial photography	0.4 m	Manual Digitisation	(1) Bare sand
Tsoar and Blumberg, 2002	Coastal	Vertical aerial photography	1.0 m – 2.0 m	Classification based on pixel brightness	(1) Vegetation
Kutiel et al., 2004	Coastal	Vertical aerial photography	Unspecified	Classification based on pixel brightness	4 landscape units
Levin and Ben-Dor, 2004	Coastal	Vertical aerial photography	Unspecified	Supervised Classification	(1) Vegetation
Hugenholtz and Wolfe, 2005	Continental	Vertical aerial photography	Unspecified	Supervised Classification	(1) Bare sand (2) Vegetation
Thomas and Leason, 2005	Continental	Satellite Landsat imagery	30 m	Field calibrated classification	4 vegetation cover classes
Hilton, 2006	Coastal	Vertical aerial photography	Unspecified	Manual Digitisation	(1) Active dune
Levin et al., 2006	Coastal	Vertical aerial photography and Landsat Satellite imagery	1 m aerial photography, 15 m Landsat Imagery	Supervised Classification (aerial photographs) and NDVI and SAVI for satellite imagery	(1) Vegetation
Wolfe et al., 2007	Continental	Vertical aerial photography	Unspecified	Supervised Classification	(1) Bare sand (2) Vegetation
Mason et al., 2008	Continental	Satellite Landsat imagery	30 m	Supervised Classification	(1) Active dune (2) Vegetated dune (3) Salt flats (4) Water (5) Dense vegetation (6) non-dune upland
Seifan, 2009	Continental	Vertical aerial photography	0.34 m – 1 m	Supervised Classification	(1) Woody vegetation (2) All other environmental entities
Jackson and Cooper, 2011	Coastal	Vertical aerial photography	1 m	Manual Digitisation	(1) Bare sand
Levin, 2011	Coastal	Vertical aerial photography and Satellite imagery	1.0 m – 2.5 m	Supervised Classification and Manual Classification	(1) Bare sand
Pye et al., 2014	Coastal	Vertical aerial photography	1 m	Classification based on pixel brightness	(1) Bare sand and thin vegetation
Ryu and Sherman, 2014	Coastal	Vertical aerial photography	< 1 m	Unsupervised and supervised classification	(1) Bare sand
Keijsers et al., 2015	Coastal	Vertical aerial photography	0.25 – 0.5 m	Supervised classification	(1) Bare Sand (2) Vegetation
Levin et al., 2017	Coastal	Vertical aerial photography	Unspecified	Supervised Classification	(1) Bare Sand (2) Vegetation
Shumack et al., 2017	Coastal	Satellite Landsat imagery	30 m	Supervised Classification	(1) Bare Sand (2) Vegetation
García-Romero et al., 2018	Coastal	Vertical aerial photography	1 m – 0.1 m	Automated classification	4 vegetation cover classes
Madurapperuma et al., 2018	Coastal	Vertical aerial photography	0.14 m – 1 m	Supervised and unsupervised classification	4 vegetation cover classes
Delgado-Fernandez et al., 2019	Coastal	Vertical aerial photography	1 m – 0.25 m	Manual Digitisation	(1) Bare sand (2) Vegetation
Jackson et al., 2019	Coastal	Satellite Landsat imagery	30 m	Supervised Classification	(1) Bare sand (2) Vegetation
Moulton et al., 2019	Coastal	Vertical aerial photography and Satellite Imagery	1 m – 5 m	Unsupervised classification and Point based manual classification	(1) Bare sand (2) Vegetated Surface
Gao et al., 2021	Coastal	Vertical aerial photography	0.2 m – 1.5 m	Supervised Classification	(1) Bare Sand (2) Vegetated Surface

The accuracy of classification in coastal dunes has been assessed using field measurements (Levin and Ben-Dor, 2004; Levin et al., 2006; Keijsers et al., 2015; Brownnett and Mills, 2017), expert assessment of aerial imagery (Madurapperuma et al., 2018; Shumack et al., 2017; Jackson et al., 2019) and a combination of sources e.g., field visits, aerial photographs, and expert opinion (Hilton, 2006). Accuracy values of remotely sensed bare sand are highly variable and range from 41% (Brownnett and Mills, 2017) to 100% at select locations (Keijsers et al., 2015; Jackson et al., 2019). This relatively large range of values may be attributed to several potential sources of error including shadows from topography and vegetation (Keijsers et al., 2015; Choi et al., 2016), wet sediment (Keijsers et al., 2015), changes in cloud cover and lighting (Delgado-Fernandez et al., 2019) and the small size of many bare sand features in dunes e.g. tracks and paths (Brownnett and Mills, 2017).

Less commonly assessed in coastal dunes has been the repeatability of remotely mapping bare sand and vegetation, however, the repeatability of remotely sensed land classification and accuracy of land cover change detection has been considered broadly within remote sensing (Olofsson et al., 2014; Khatami et al., 2016; Lyons et al., 2018). In addition, few studies have assessed the effect of different classification methods or image resolutions on either classification accuracy or estimated extent on coastal dunes (Keijsers et al., 2015; Choi et al., 2016; Madurapperuma et al., 2018). Given the increased accessibility of high-resolution satellite data and UAV images, and associated consideration of dune dynamics from such data, there is an increased need to understand the accuracy and repeatability of the data derived from remote sensed vegetation/bare sand classification. This study evaluates the accuracy and repeatability of remotely sensing bare sand and vegetation in a temperate coastal dune. To represent the breadth of research previously conducted, areas of bare sand and vegetation were mapped using a range of image resolutions and classification techniques.

Study site

In this study we focused on quantifying the area covered by bare sand and vegetation on a coastal sand dune in Ynyslas, part of the Dyfi National Nature Reserve on the west coast of Wales ($52^{\circ}31'54.8''N$ $4^{\circ}03'06.4''W$) (Fig. 1). Field data was collected on 5th February 2020 on a discrete coastal sand dune at the northern distal end of a spit which extends into the lower Dyfi estuary (Fig. 1). The sand dune has grown from a patch of nebkha dune that formed in 2006 as evidenced from aerial imagery and field description by Nield et al. (2011). Aerial imagery of the site demonstrated that the spatial area of the dune (outlined in Fig. 1) remained relatively constant between 2015 and the field survey in February 2020, maintaining an area of approximately 8000 m². At the time of the study (February 2020), the sand dune had a maximum elevation of 5 m relative to the surrounding beach and spatial changes in elevation on the dune (i.e. slope) were generally gradual apart from a steep dune scarp along the north eastern extent of the dune caused by frequent marine erosion (Fig. 1). Vegetation on the dune was dominated by marram grass *Ammophila arenaria* (L.).

Methods

The methods comprise of four main steps, 1) collection of aerial imagery, 2) field survey of land cover, 3) image classification and 4) comparison of measured and modelled data.

Aerial imagery collection

RGB aerial imagery was collected using a DJI Mavic Pro 2 uncrewed aerial vehicle (UAV). The flight was planned using Pix4DCapture based on a ground pixel resolution of 0.01 m. Lateral and longitudinal overlap was set to 80%. Prior to flying, eight (5.8 per 100 photos) Ground

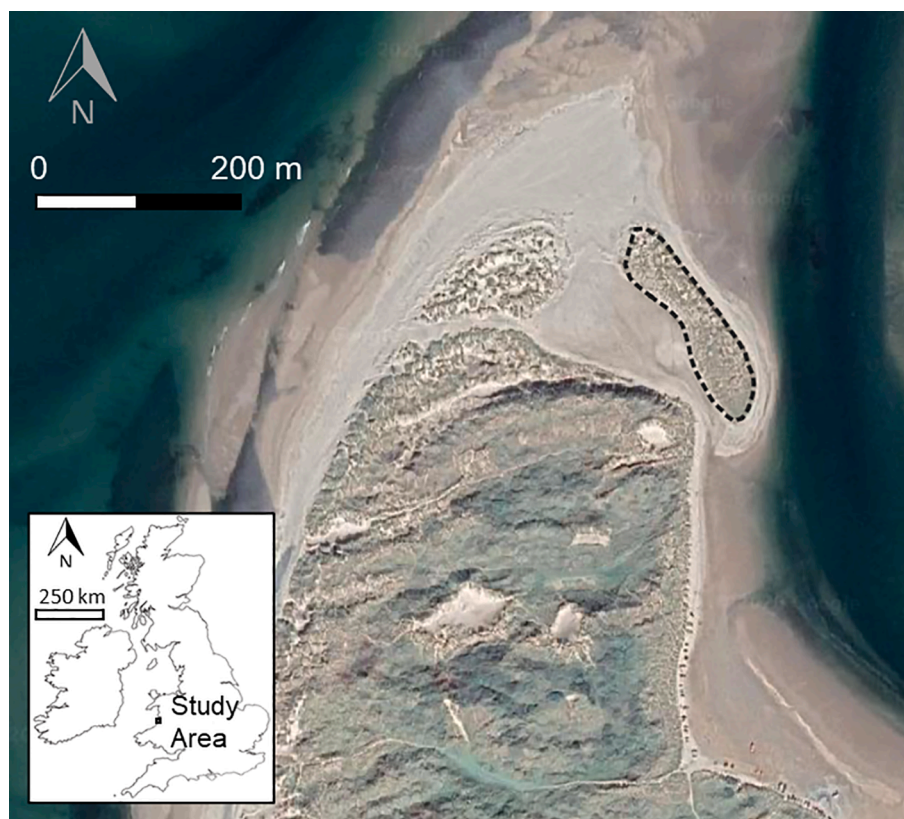


Fig. 1. Aerial image of the northern distal end of Ynyslas sand dunes, part of the Dyfi National Nature Reserve on the west coast of Wales ($52^{\circ}31'54.8''N$ $4^{\circ}03'06.4''W$) taken on 18th September 2019. The black dashed line denotes the area in which sand and vegetation was mapped (Image Source: Google Earth).

Control Points (GCPs) were evenly distributed throughout the dune and their location surveyed using a Trimble R8 differential global positioning system (DGPS). Orthorectification and mosaicking of the aerial imagery collected was performed using Pix4Dmapper utilising a fully automated workflow based on Structure-from-Motion (SFM) digital photogrammetry algorithms (see Chesley et al., 2017). Before initiating this workflow, Pix4Dmapper was also used to manually identify the surveyed GCPs within the aerial imagery. By comparing the absolute coordinates of the GCPs surveyed with those for the same location within the resulting orthomosaic, a root mean square error of 0.003 m was calculated in the X, Y and Z directions, respectively, indicating a high degree of relative accuracy. The orthomosaic image was subsequently resampled to resolutions of 10 m, 3 m, 1 m and 0.25 m to represent a range of digital imagery products commonly used for dune vegetation classification (Fig. 2 and Table 2).

Table 2

Image pixel resolutions associated with a range of digital aerial imagery products.

Product	Pixel Size
Sentinel-2 (Satellite)	10 m
PlanetScope (Satellite)	3.125 m
Aerial Imagery (Plane)	0.25 m, 1 m
Aerial Imagery (UAV)	0.01 m

Land cover survey

To assess the accuracy of remotely sensed classifications, ground truth samples of the study area were collected on 5th February 2020 immediately after the uncrewed aerial vehicle was flown. Each sampling unit measured 0.25 m × 0.25 m and was located at random within the study area (Fig. 1). Data collection continued until at least 50 samples of

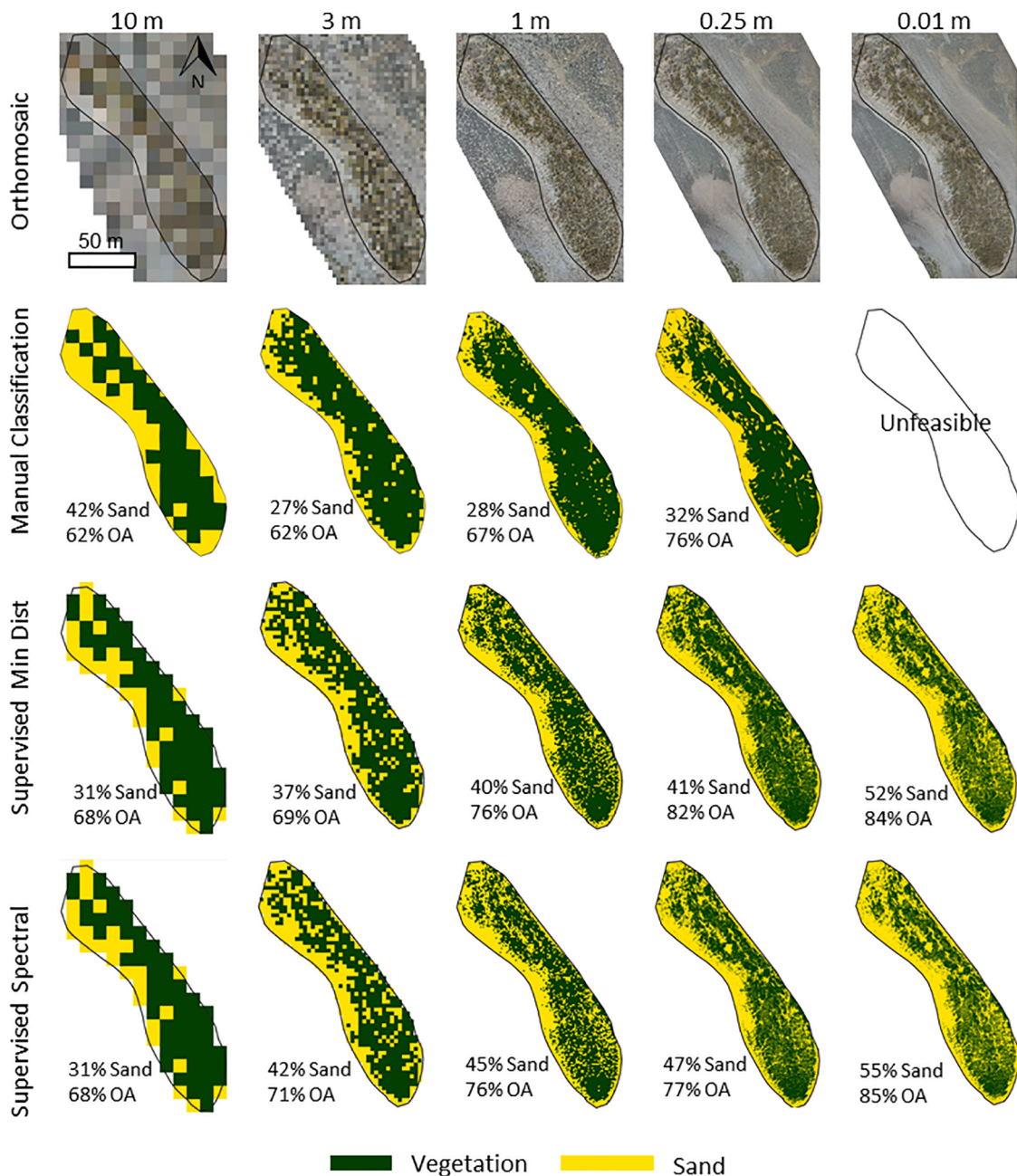


Fig. 2. Orthomosaic images of study site and mapped classifications of vegetation and bare sand for replicate 1. OA = Observed Agreement.

each land classification (1. Vegetation 2. Sand) were measured (Congalton and Green, 2019). The centre of each sampling location was identified in the field using the 'stake out' function on a Trimble R8 differential global positioning system. At each location, the vegetation cover %, presence of 'yellowed' vegetation (yes or no) and presence of a steep slope (defined as $< 35^\circ$) (yes or no) was recorded. A unit was classified as vegetated if it had a vegetation cover of $\geq 50\%$ and sand if it had a vegetation cover of $< 50\%$, thus creating a binary classification. Data collected in the field was cross referenced with digital ground photographs taken at each location to reduce potential transcription error in the field.

Image classification

For each image resolution, land classification was performed by both manual digitisation and by semi-automatic, supervised classification. Manual classification was performed by digitising areas of bare sand as polygons in the desktop geographic information system, QGIS (v3). The areas not manually digitised as bare sand within the study area were assumed to be vegetated, analogous to the approach applied by Delgado-Fernandez et al. (2019). The manual classification of 0.01 m resolution imagery was not attempted as accurate manual classification of bare sand and vegetation at this resolution was deemed unfeasible.

Supervised classification was completed in QGIS using the semi-automatic classification plugin (SCP) (Congedo, 2016). Classification was performed using the minimum distance and spectral angle mapping algorithms using true-colour RGB images. Classification was also performed using manual classification and minimum distance for a 1 m resolution single-band grayscale image. Minimum distance calculates the mean spectra of each predefined class and assigns a pixel to a class that has the least distance to the mean (Mather and Tso, 2016). Spectral angle mapping calculates the spectral angle between spectral signatures of images pixels and training spectral signatures. In spectral angle mapping a pixel belongs to the class to which it has the lowest angle (Kruse et al., 1993).

Classification at each image resolution was trained using 40 regions of interest (ROIs): 20 regions of interest represented vegetation and 20 regions of interest represented bare sand. A total of 40 regions of interest were used as this was the maximum that could be selected in the 10 m resolution image. Training data was not shared between classifications but conducted independently for each and every classification. Regions of interest were selected to best represent the range of colours seen in each class. The total area of training samples for each replicate varied on average by 30% (relative standard deviation) for colour image classifications and 7% for the grayscale classifications. Training samples were approximately evenly distributed across the mosaic. No radiometric correction of images was performed as all aerial photographs were taken in analogous lighting conditions (6-minute flight time). Both manual and semi-automatic classifications were conducted by the same analyst three times for each image resolution including training. Classifications were also made in the same order i.e. from lowest resolution image (10 m pixel) to highest (0.01 m pixel).

Comparison of measured and modelled data

Comparison of remotely sensed and ground-truth samples were performed for all three iterations of each classification method and resolution (42 RGB classifications and 6 grayscale classifications). The classification of each location was calculated from a 0.25×0.25 m quadrat, identical to the location measured in the field. A quadrat was classified as vegetated if it had a vegetation cover of $\geq 50\%$ and sand if it had a vegetation cover of $> 50\%$ replicating the method used in the field survey. A classification was deemed correct if the binary remotely sensed land classification polygon and ground truth classification agreed. The results of each classification were analysed by calculating the percentage agreement (overall accuracy) and kappa coefficient,

user's accuracy and producer's accuracy. The kappa coefficient is an overall accuracy parameter that takes into account whether samples were mapped correctly by chance. Landis and Koch (1977) proposed a scale whereby a value of < 0.00 = poor agreement, $0.00 - 0.20$ = slight agreement, $0.21 - 0.40$ = fair agreement, $0.41 - 0.60$ = moderate agreement, $0.61 - 0.80$ = substantial agreement and $0.81 - 1.00$ = almost perfect agreement. User's accuracy represents the probability for a given class that a pixel chosen on the map represents that category on the ground, and producer's accuracy is the probability that random location chosen in the field has the same class value as that on a map.

Results

% bare sand cover

When considering all replicates and resolutions of the colour imagery, an average of 31% of the study area was mapped as bare sand by manual classification, compared to 44% for minimum distance supervised classification and 47% for spectral angle mapping supervised classification (Table 3). For the coarsest resolution image (10 m), all three classification methods recorded a very similar area of bare sand (33% – 34%), however for 3 m and 1 m image resolutions the area mapped as bare sand by manual classification decreased below 30%, while the area of bare sand mapped by supervised classification methods increased to over 40% (Fig. 4). Both supervised classification methods show a trend of increasing bare sand area as pixel size decreases from 10 m to 0.25 m. However, for 0.01 m resolution image, the average area of bare sand mapped by both supervised classification methods decreased (Fig. 4).

Regarding variation between replicates, on average the area of bare sand mapped by manual classification was less variable (average range of 5%) than the supervised classification methods, which both had an average range of 10%. Fig. 3 demonstrates that the variation in classification between replicates occurred throughout the study area. For manual classification, the 10 m image resolution exhibited the largest range (15%) between replicates and the 3 m resolution data the smallest (1%). For supervised classification methods, the 0.25 m resolution image generated the largest range of mapped bare sand for both minimum distance and spectral angle supervised classification (20%). The 3 m resolution image produced the smallest range (5%) for minimum distance supervised classification and the 10 m and 1 m images produced the smallest variation in sand for the spectral angle mapping supervised classification (both 6%) (Table 3 and Fig. 3).

Observed agreement

Observed agreement between ground truth classification and remotely sensed classification generally increased as image resolution increased (i.e., a decrease in pixel size). This trend was observed for all classification methodologies tested (Fig. 5 and Table 3). When considering all colour image replicates and resolutions, on average, manual classification recorded a poorer observed agreement (69%) than minimum distance and spectral angle supervised classification (both had an average of 76%). The lowest observed agreement was 64% for the 3 m resolution image using the manual classification method, 1% lower than the observed agreement percentage for manual classification of the 10 m image (Fig. 5 and Table 3). The highest observed agreement was 84% for the 0.01 m image, mapped using spectral angle mapping supervised classification. The kappa coefficient, which takes into consideration whether samples were mapped correctly by chance, ranges from a fair agreement, which is calculated for all classification methods using the 10 m resolution image, to substantial agreement for the supervised classification of the 0.25 m and 0.01 m resolution images (Fig. 5).

The percentage of observed agreement demonstrated less variation between replicates than the percentage area of sand mapped. On average minimum distance supervised classification had the smallest

Table 3

Summary of percentage bare sand cover mapped within the study site, observed agreement and kappa coefficient for manual digitisation, minimum distance supervised classification (MinDist) and spectral angle mapping (Sp) supervised classification.

Replicate no.	% Bare Sand Cover				Observed Agreement %				Kappa Coefficient				Description
	1	2	3	Av.	1	2	3	Av.	1	2	3	Av.	
Manual 10 m	42	32	27	34	62	64	68	65	0.24	0.28	0.36	0.29	Fair
Manual 3 m	27	27	28	27	62	66	63	64	0.25	0.33	0.27	0.28	Fair
Manual 1 m	28	27	31	28	67	71	72	70	0.35	0.42	0.42	0.40	Fair
Manual 0.25 m	32	33	34	33	76	75	76	76	0.52	0.5	0.52	0.51	Moderate
Min Dist 10 m	31	31	37	33	69	69	72	70	0.39	0.39	0.43	0.40	Moderate
Min Dist 3 m	37	42	41	40	69	71	71	70	0.38	0.42	0.42	0.41	Moderate
Min Dist 1 m	40	46	41	42	76	75	76	76	0.52	0.5	0.52	0.51	Moderate
Min Dist 0.25 m	41	61	60	54	82	82	82	82	0.64	0.64	0.64	0.64	Substantial
Min Dist 0.01 m	53	42	52	49	83	83	83	83	0.66	0.66	0.66	0.67	Substantial
Spectral 10 m	31	33	37	34	69	67	72	69	0.39	0.35	0.43	0.39	Fair
Spectral 3 m	42	49	47	46	71	72	72	72	0.42	0.44	0.44	0.43	Moderate
Spectral 1 m	45	50	44	47	76	77	76	76	0.52	0.54	0.52	0.53	Moderate
Spectral 0.25 m	47	67	63	59	78	80	83	80	0.56	0.6	0.66	0.61	Substantial
Spectral 0.01 m	55	44	54	51	82	83	83	83	0.64	0.66	0.68	0.66	Substantial

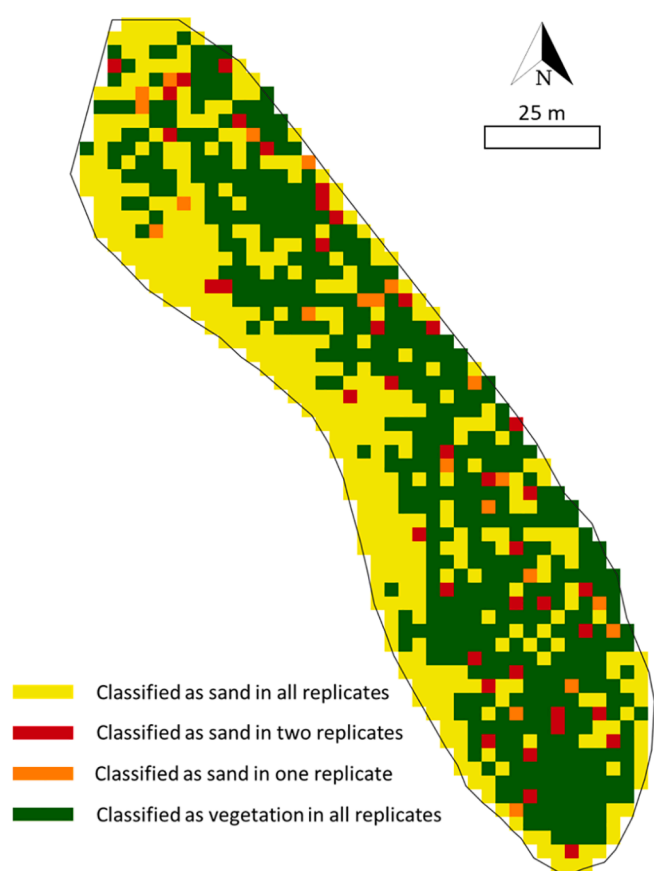


Fig. 3. Classification difference map for all 3 replicates using the 3 m resolution image and the spectral angle mapping supervised classification method.

variation (minimum distance 1%, spectral mapping 3%) and manual classification the greatest (4%). For manual classification, variation in observed agreement decreased as image resolution increased from an average of 6% for the 10 m image to 2% for the 0.25 m image (Fig. 5). No clear trend between image resolution and the variability in the percentage observed agreement for supervised classification methods was observed. For example, the 0.25 m resolution image exhibited no variation between replicates for minimum distance supervised classification but a range of 5% for the spectral mapping supervised classification at the same image resolution (Table 3).

User's and Producer's accuracy

Fig. 6 and Table 4 demonstrate that user and producer accuracies generally increased with image resolution (i.e. smaller pixel size). Sand had the greatest variability in user's accuracy whereby manual classification reported substantially lower accuracy values than for both automated classifications, indicating that manual classification underestimates the area of bare sand, particularly at higher image resolutions. The producer accuracy of vegetation was also consistently lower than the automated classification for each image resolution investigated.

Grayscale 1 m aerial images

The percentage of the study area manually classified as bare sand in the 1 m grayscale image was substantially lower than that measured in the true colour image (15% and 28% respectively) (Fig. 7a). Similarly, the percentage agreement of the manual classification with the observed data fell from 70% agreement for the colour image, to 61% for the grayscale image (Fig. 7b). The kappa coefficient descriptor remained 'fair' but declined from an average of 0.40 for the colour manual classification to 0.24 for the grayscale manual classification. In contrast to the discrepancy between the manual classification of the colour and grayscale images, the range and average percentage of the area classified as bare sand using the supervised minimum classification method differed by only 1% (Fig. 7a). The average percentage agreement between the 1 m colour and grayscale image also only differed by 1% and the average kappa coefficient for both was described as moderate (0.53 for grayscale and 0.51 for colour).

Consistently incorrect classification locations

In order to identify the environmental conditions where remote sensing of bare sand and vegetation is most likely to be erroneous, the 13 locations at which land cover type was incorrectly classified for the 0.01 m resolution colour image are summarised in the Table 5. Table 5 shows that at 9 of the 13 locations the percentage of observed vegetation was within $\pm 10\%$ of the threshold classification value (50%). This indicates that classification may be prone to error at those locations where vegetation cover is relatively close to the threshold classification value. Locations 29 and 40 also further demonstrate how remotely sensed classifications of bare sand may mistake 'yellowing' and seemingly 'dead' vegetation for areas of sand.

Discussion

This study assessed how the extent and accuracy of remotely sensed areas of bare sand and vegetation in dunes varied with image resolution

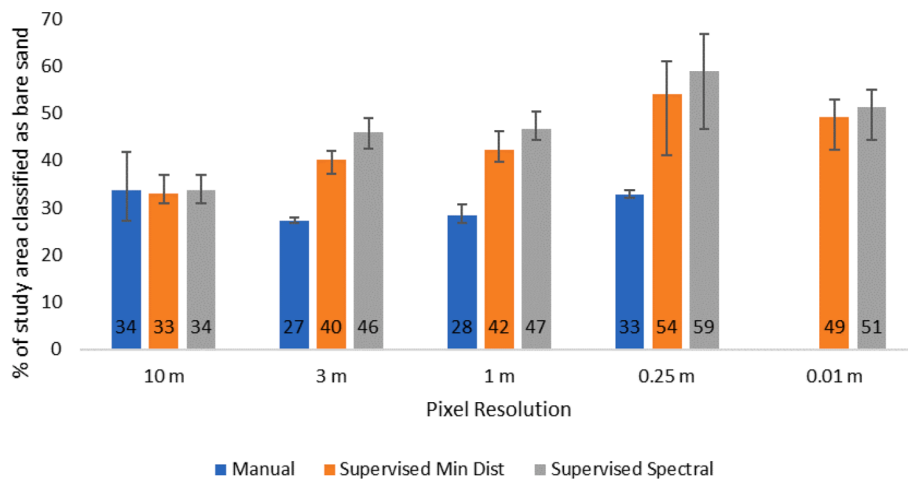


Fig. 4. Average percentage bare sand coverage calculated for each image pixel resolution and classification method using true colour imagery. Error bars represent maximum and minimum values from three replicates (Table 3).

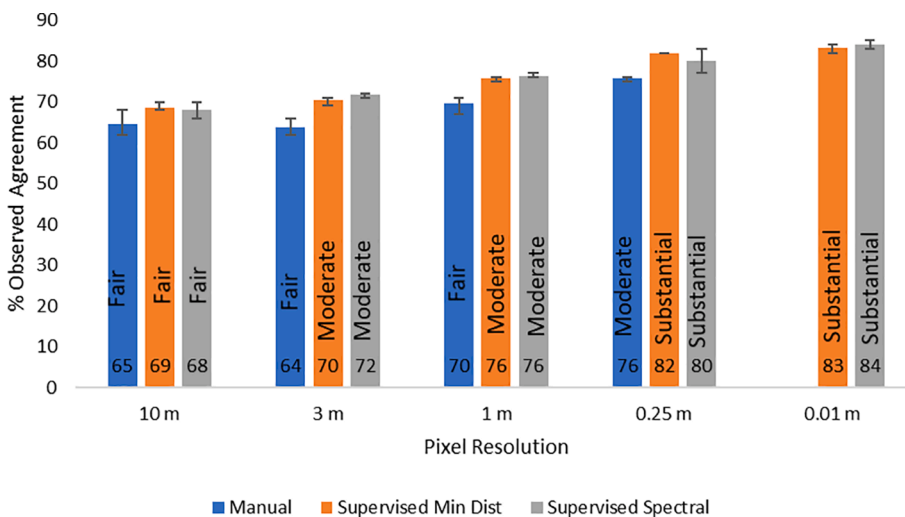


Fig. 5. Average percentage observed agreement calculated for each image pixel resolution and classification method using true colour imagery. Error bars represent maximum and minimum values from three replicates (Table 3). Text descriptors refer to the average kappa coefficient, whereby < 0.00 = poor agreement, 0.00 – 0.20 = slight agreement, 0.21 – 0.40 = fair agreement, 0.41 – 0.60 = moderate agreement, 0.61 – 0.80 = substantial agreement and 0.81 – 1.00 = almost perfect agreement (Table 3).

and classification methodology. Supervised methods of classification (semi-automatic) mapped a greater extent of bare sand and were more accurate than manual digitisation but had poorer repeatability. For all classification methodologies, observed agreement with field data generally increased with image resolution (i.e. smaller pixel size). It must however be considered that the study area examined was a relatively simple landscape compared to some other coastal dune landscapes where a larger number of land cover classifications may be present (e.g. water, shrubs, forest, pathways) and geomorphic features such as blowouts and steep erosional walls may create shadowing, making accurate remotely sensed classification difficult (e.g. Fig. 2 and Fig. 6 in Smyth et al., 2020).

The results from the classification of the 1 m resolution grayscale and true-colour images show little difference in the percentage of bare sand recorded or the percentage observed agreement using minimum distance supervised classification, however the manual classification of the 1 m resolution grayscale image recorded substantially lower bare sand than the classification of the colour image (Fig. 7a) and had a lower percentage observed agreement than the colour image (Fig. 7b). The resemblance between the classification of grayscale and colour images using supervised classification concur with the findings of Keijsers et al. (2015) who converted colour images to grayscale as it had little difference on the classification results but reduced the computational time of the classification process. The decline in performance of manual

classification in grayscale imagery is likely due to the increased conservatism of the analyst when selecting areas of bare sand resulting in a larger proportion of the study area being classified as vegetation. Our findings suggest that the additional information provided by multiple colour channels (e.g. RGB) aids the analyst in more accurately delineating bare sand in manual classification.

The considerable variation in the mapped extent of bare sand and vegetation between replicates (Table 3) indicates that both manual and supervised classification methods are subject to substantial repeatability error i.e., the variability in the measurements made using the same method, data and analyst can only be ascribed to errors due to the measurement process itself (Bartlett and Frost, 2008). The relatively large repeatability errors measured in this study stem from the subjective elements present in all the methodologies tested i.e., the selection of bare sand in manual classification and the selection of training regions of interest in supervised classifications. This further highlights Foody’s (2002) recommendation that analysts should extensively define all classes within the study area, even if they are of no interest. When selecting reference polygons analysts must also be conscious of selecting samples that are bias toward sand or vegetation of a particular colour and that reference polygons from outside the study area may also be needed (Zhen et al., 2013). Accurate landcover delineation in coastal dunes is particularly difficult as the visual appearance of bare sand can be highly variable due to changes in mineral content and moisture

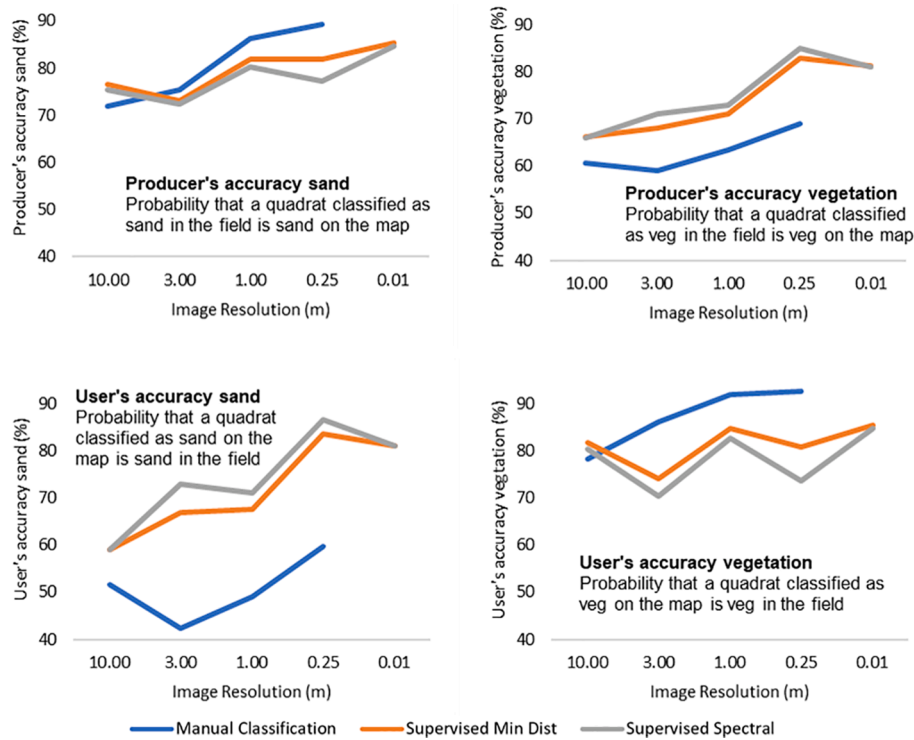


Fig. 6. Producer's and user's accuracy for sand and vegetation.

Table 4
Producer's and user's accuracy for sand and vegetation.

Replicate no.	Producer's Accuracy Sand				Producer's Accuracy Vegetation				User's Accuracy Sand				User's Accuracy Vegetation			
	1	2	3	Av	1	2	3	Av	1	2	3	Av	1	2	3	Av
Manual 10 m	65	70	81	72	60	60	62	61	55	51	49	52	69	78	88	78
Manual 3 m	74	77	75	75	58	61	58	59	39	47	41	42	86	86	86	86
Manual 1 m	85	87	87	86	61	64	65	63	43	51	53	49	92	92	92	92
Manual 0.25 m	86	91	91	89	70	68	69	69	63	57	59	60	90	94	94	93
Min Dist 10 m	77	77	76	77	65	65	69	66	56	56	65	59	83	83	79	82
Min Dist 3 m	73	73	73	73	66	69	69	68	63	69	69	67	76	73	73	74
Min Dist 1 m	83	80	83	82	71	71	71	71	67	69	67	68	86	82	86	85
Min Dist 0.25 m	88	79	79	82	77	86	86	83	75	88	88	84	90	76	76	81
Min Dist 0.01 m	83	90	83	85	83	78	83	81	84	75	84	81	82	92	82	85
Spectral 10 m	77	73	76	75	65	64	69	66	56	56	65	59	83	79	79	80
Spectral 3 m	73	72	72	72	69	72	72	71	69	75	75	73	73	69	69	70
Spectral 1 m	81	79	81	80	72	75	72	73	69	75	69	71	84	80	84	83
Spectral 0.25 m	78	75	79	77	78	89	88	85	78	92	90	87	78	67	76	74
Spectral 0.01 m	81	90	83	85	83	78	82	81	84	75	84	81	80	92	82	85

(Fig. 8a). The large range in visual appearance may result in 'dark' patches of sand being mistakenly classified as vegetation (Fig. 8b). Vegetation can be more easily discriminated from dark sand/soil using near infra-red (NIR) data available from both the PlanetScope and Sentinel-2 sensors (Table 2) and classifiers such as random forest may also be more suited to classifying heterogeneous environments such as coastal sand dunes (Belgiu and Drăguț, 2016). Fig. 8 also demonstrates how the visual appearance of vegetation can also be highly variable, with patches of dead vegetation that are light in colour, being mistakenly classified as bare sand. Distinguishing non-photosynthetic vegetation (dry or dead vegetation) from bare ground is often difficult without hyperspectral data, as each classes spectral response is similar (Li and Guo, 2016).

To date, explicit appreciation of repeatability has been absent from research examining bare sand and vegetation dynamics in dunes. Despite this, the key findings of many previous studies are unlikely to be impacted. This is either because the change in land cover extent has been so large (e.g. an average reduction in bare sand area of 81% (Pye et al.,

2014)) or bare sand extent was classified manually (e.g. Jackson and Cooper, 2011; Delgado-Fernandez et al., 2019), a method which our results demonstrate to be a more repeatable but less accurate method than supervised classification. The poor repeatability of supervised classification methodologies should however be considered in future studies that analyse change detection (e.g. Hugenholtz and Wolfe, 2005), compare images of various resolutions (e.g. Tsoar and Blumberg, 2002; Seifan, 2009; Levin, 2011; Delgado-Fernandez et al., 2019) and in studies that include relatively small ($\pm 10\%$) seasonal or annual vegetation changes. The errors identified in this study should also be taken into consideration when remote sensing is used to report on the conservation status and condition of sand dunes (Brownnett and Mills, 2017).

As well as a substantial discrepancy in the repeatability of manual and supervised classifications, Fig. 4 demonstrates that for all image resolutions, supervised classification estimated a larger extent of bare sand compared to manual classification and had a greater agreement when compared to ground-truthing performed in the field (Table 3 and Fig. 5). This discrepancy between manual and supervised classification,

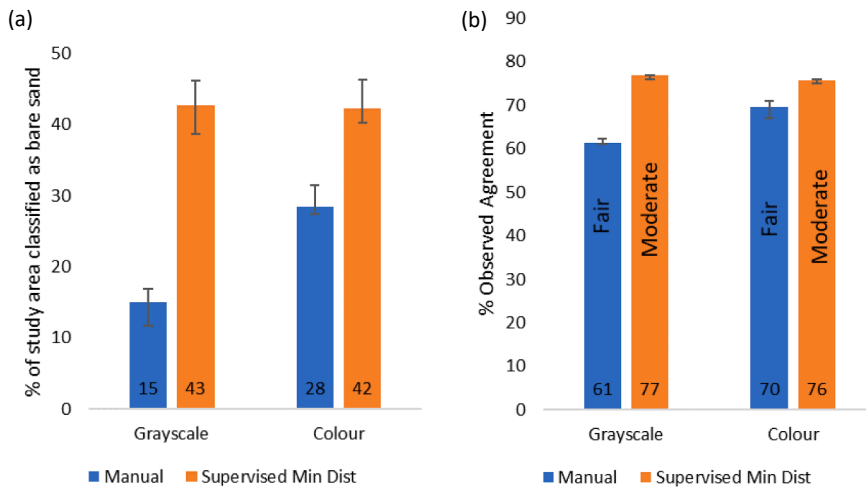


Fig. 7. (a) Average % of study area classified as bare sand from the 1 m resolution grayscale image using manual and minimum distance classification. Error bars represent maximum and minimum values from three replicates. (b) % observed agreement for the 1 m resolution grayscale image. Error bars represent maximum and minimum values from three replicates (Table 3). Text descriptors refer to the average kappa coefficient, whereby < 0.00 = poor agreement, 0.00 – 0.20 = slight agreement, 0.21 – 0.40 = fair agreement, 0.41 – 0.60 = moderate agreement, 0.61 – 0.80 = substantial agreement and 0.81 – 1.00 = almost perfect agreement (Table 3).

Table 5
Random sample locations at which the remotely sensed classification and the observed classification disagreed for all the replicates of the 0.01 m resolution image mapped using spectral angle mapping supervised classification.

Location no.	% observed vegetation in 0.25 m ² sample	Dead vegetation (y/n)	Steep slope (y/n)	Notes	Remotely sensed classification
4	15			In between 2 canopies	Vegetation
24	40	y		Dead at ground. Living canopy	Vegetation
29	55	y		Dead	Bare Sand
40	75	y		Dead	Bare Sand
46	60				Bare Sand
55	40				Vegetation
56	65			Very close to path	Bare Sand
64	45				Vegetation
72	20				Bare Sand
84	45		y	Steep slope	Vegetation
95	52				Bare Sand
99	45				Vegetation
104	45				Vegetation

which is particularly distinct at finer resolutions (Fig. 4), may be caused by the increased ability of automated detection to classify small areas of bare surface within areas that are uniformly classified as vegetated in

manual classification (Fig. 2). Comparisons between the bare sand extent reported by different studies, image resolutions and classification methods should therefore be considerate of the relatively large potential for error. For example, the results from this study indicate that manual classification may underestimate bare sand extent by as much as 26% (the difference in the average bare sand extent between manual and spectral angle mapping supervised classification for the 0.25 m resolution image). This underestimation has however been calculated in a specific environmental setting and may not be expected in all cases. As the data from this study demonstrates that incorrect classification is most prevalent in heterogeneous environments where the vegetation cover was near to 50% ($\pm 10\%$) in the sampled quadrat, land cover classification may be more accurate in areas with sharp boundaries between dense vegetation and active dune sand e.g. parabolic dunes, blowouts and large sand sheets (Hugenholtz and Wolfe, 2005; Delgado-Fernandez et al., 2018) as well as in arid environments where vegetation is less ubiquitous (García-Romero et al., 2018). However, complex patterns of vegetation and substrates are still common in arid coastal environments (García-Romero et al., 2018), desert dunes (Levin et al., 2012), incipient foredunes (Nolet et al., 2018) and continental dunes (Marín et al., 2005; Seifan, 2009).

The results in Figs. 5 and 6 indicate that as image resolution increases so too does observed agreement, users accuracy and producers accuracy. This improvement in agreement between remotely-sensed and ground based measurements is due to the decrease in spectral mixing that occurs as pixel size decreases, i.e. the range of surfaces reflected in a single pixel (e.g. sand, vegetation and dead biomass), decreases as a pixel becomes smaller resulting in a less ‘mixed pixel’ (Hugenholtz et al., 2012). The manner in which pixel spectral values become increasingly mixed with

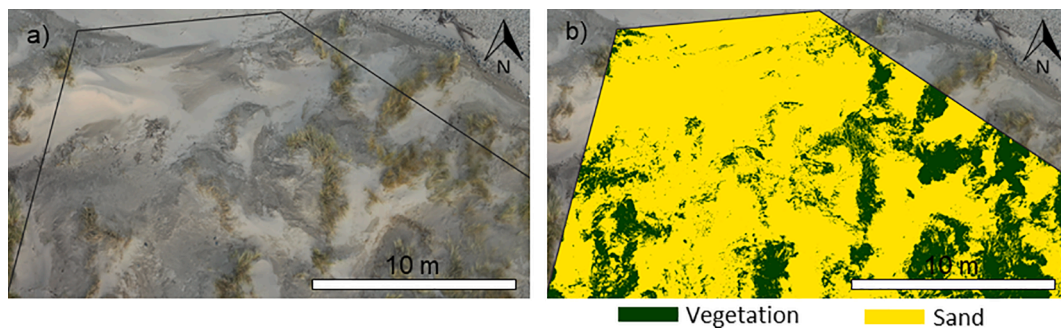


Fig. 8. (a) 0.01 m orthomosaic demonstrating the highly variable visual properties of both bare sand and vegetation present within the study site, (b) iteration 1 of spectral angle mapping supervised classification for 0.01 m resolution orthomosaic. The solid black line in both images indicates the extent of the study area.

pixel size is clearly visible in Fig. 2, particularly for the 10 m and 3 m images. For studies using these ‘medium’ image resolutions, use of spectral unmixing or regression techniques that measure vegetation as a continuous value rather than a binary classification may be useful (Ettritch et al., 2018). Errors may still occur at very high image resolutions e.g. 0.01 m pixel size, as accurate identification of sand by manual classification and in the training samples for semi-automated classification methods becomes unfeasible due to the level of detail presented in the image and the time taken to identify/remove a greater range of artefacts that are not focus of the research e.g. litter, wrack and shadow. To further improve classification, future studies could implement a resampling approach (e.g. Monte Carlo, bootstrapping) with a large number iterations giving a distribution of area estimates (Lyons et al., 2018) and statistically calculate the standard error for a classified area (see Olofsson et al., 2014).

Conclusion

Remote sensing of bare sand and vegetation in dunes requires careful consideration of the classification method, image resolution and selection and number of training samples. The results from this research support the use multiple replicates when mapping bare sand as this data can be used to report a range of values and potential error. Where multiple replicates are not used and in dunes where a complex mosaic of bare sand and vegetation exists, specific reference to the potential sources and range of error should be considered regardless of the classification methods used.

Declaration of Competing Interest

The authors declare that they have no known competing financial interests or personal relationships that could have appeared to influence the work reported in this paper.

Acknowledgements

We wish to thank Justin Lyons and Natural Resources Wales for generously facilitating access to the field site. This work was funded through the UK Natural Environment Research Council grant NE/T00410X/1. The global positioning system used in the study was funded by the Royal Society grant RG170467.

References

- Arens, S.M., De Vries, S., Geelen, L.H., Ruessink, G., van der Hagen, H.G., Groenendijk, D., 2020. Comment on ‘Is ‘re-mobilisation’ nature restoration or nature destruction? A commentary’ by I. Delgado-Fernandez, RGD Davidson-Arnott & PA Hesp. *J. Coast. Conserv.* 24 (2), 1–4.
- Bartlett, J.W., Frost, C., 2008. Reliability, repeatability and reproducibility: analysis of measurement errors in continuous variables. *Ultrasound Obstet. Gynecol.* 31 (4), 466–475.
- Belgiu, M., Drăguț, L., 2016. Random forest in remote sensing: A review of applications and future directions. *ISPRS J. Photogramm. Remote Sens.* 114, 24–31.
- Brownett, J.M., Mills, R.S., 2017. The development and application of remote sensing to monitor sand dune habitats. *J. Coast. Conserv.* 21 (5), 643–656.
- Chesley, J.T., Leier, A.L., White, S., Torres, S., 2017. Using unmanned aerial vehicles and structure-from-motion photogrammetry to characterize sedimentary outcrops: An example from the Morrison Formation, Utah, USA. *Sed. Geol.* 354, 1–8.
- Choi, S.K., Lee, S.K., Jung, S.H., Choi, J.W., Choi, D.Y., Chun, S.J., 2016. Estimation of fractional vegetation cover in sand dunes using multi-spectral images from fixed-wing UAV. *한국측량학회지* 34 (4), 431–441.
- Congalton, R.G., Green, K., 2019. *Assessing the Accuracy of Remotely Sensed Data: Principles and Practices*. CRC Press.
- Congedo, L., 2016. Semi-automatic classification plugin documentation. Release 4 (0.1), 29.
- Curr, R.H.F., Koh, A., Edwards, E., Williams, A.T., Davies, P., 2000. Assessing anthropogenic impact on Mediterranean sand dunes from aerial digital photography. *J. Coast. Conserv.* 6 (1), 15–22.
- De Battisti, D., Griffin, J.N., 2020. Below-ground biomass of plants, with a key contribution of buried shoots, increases foredune resistance to wave swash. *Ann. Bot.* 125 (2), 325–334.
- Delgado-Fernandez, I., Smyth, T.A., Jackson, D.W., Smith, A.B., Davidson-Arnott, R.G., 2018. Event-scale dynamics of a parabolic dune and its relevance for mesoscale evolution. *J. Geophys. Res. Earth Surf.* 123 (11), 3084–3100.
- Delgado-Fernandez, I., O’Keeffe, N., Davidson-Arnott, R.G., 2019. Natural and human controls on dune vegetation cover and disturbance. *Sci. Total Environ.* 672, 643–656.
- Ettritch, G., Bunting, P., Jones, G., Hardy, A., Nagendra, H., He, K., 2018. Monitoring the coastal zone using earth observation: application of linear spectral unmixing to coastal dune systems in Wales. *Remote Sens. Ecol. Conserv.* 4 (4), 303–319.
- Feagin, R.A., Furman, M., Salgado, K., Martinez, M.L., Innocenti, R.A., Eubanks, K., Figlus, J., Huff, T.P., Sigren, J., Silva, R., 2019. The role of beach and sand dune vegetation in mediating wave run up erosion. *Estuar. Coast. Shelf Sci.* 219, 97–106.
- Foody, G.M., 2002. Hard and soft classifications by a neural network with a non-exhaustively defined set of classes. *Int. J. Remote Sens.* 23 (18), 3853–3864.
- Gao, J., Kennedy, D.M., Konlechner, T.M., 2020. Coastal dune mobility over the past century: a global review. *Prog. Phys. Geogr.: Earth Environ.* 0309133320919612.
- Gao, J., Kennedy, D.M., Konlechner, T.M., McSweeney, S., Chiaradia, A., McGuirk, M., 2021. Changes in the vegetation cover of transgressive dune fields: A case study in Cape Woolamai, Victoria. *Earth Surf. Process. Landforms*.
- García-Romero, L., Hernández-Cordero, A.I., Hernández-Calvento, L., Espino, E.P.C., López-Valcarcel, B.G., 2018. Procedure to automate the classification and mapping of the vegetation density in arid Aeolian sedimentary systems. *Prog. Phys. Geogr.: Earth Environ.* 42 (3), 330–351.
- Hilton, M.J., 2006. The loss of New Zealand’s active dunes and the spread of marram grass (*Ammophila arenaria*). *N. Z. Geogr.* 62 (2), 105–120.
- Hilton, M., Duncan, M., Jul, A., 2005. Processes of *Ammophila arenaria* (marram grass) invasion and indigenous species displacement, Stewart Island, New Zealand. *J. Coastal Res.* 21 (1), 175–185.
- Hughenoltz, C.H., Levin, N., Barchyn, T.E., Baddock, M.C., 2012. Remote sensing and spatial analysis of aeolian sand dunes: A review and outlook. *Earth Sci. Rev.* 111 (3–4), 319–334.
- Hughenoltz, C.H., Wolfe, S.A., 2005. Recent stabilization of active sand dunes on the Canadian prairies and relation to recent climate variations. *Geomorphology* 68 (1–2), 131–147.
- Jackson, D.W.T., Cooper, J.A.G., 2011. Coastal dune fields in Ireland: rapid regional response to climatic change. *J. Coastal Res.* 293–297.
- Jackson, D.W., Costas, S., González-Villanueva, R., Cooper, A., 2019. A global ‘greening’ of coastal dunes: An integrated consequence of climate change? *Global Planet. Change* 182.
- Keijsers, J.G.S., De Groot, A.V., Riksen, M.J.P.M., 2015. Vegetation and sedimentation on coastal foredunes. *Geomorphology* 228, 723–734.
- Khatami, R., Mountrakis, G., Stehman, S.V., 2016. A meta-analysis of remote sensing research on supervised pixel-based land-cover image classification processes: General guidelines for practitioners and future research. *Remote Sens. Environ.* 177, 89–100.
- Kruse, F.A., Lefkoff, A.B., Boardman, J.W., Heidebrecht, K.B., Shapiro, A.T., Barloon, P. J., Goetz, A.F.H., 1993. The spectral image processing system (SIPS)-interactive visualization and analysis of imaging spectrometer data. No. 1. In: *AIP Conference Proceedings*. American Institute of Physics, pp. 192–201.
- Kutieli, P., 2001. Conservation and management of the Mediterranean coastal sand dunes in Israel. *J. Coast. Conserv.* 7 (2), 183–192.
- Kutieli, P., Cohen, O., Shoshany, M., Shub, M., 2004. Vegetation establishment on the southern Israeli coastal sand dunes between the years 1965 and 1999. *Landscape Urban Plann.* 67 (1–4), 141–156.
- Landis, J.R., Koch, G.G., 1977. The measurement of observer agreement for categorical data. *Biometrics* 33 (1), 159.
- Levin, N., 2011. Climate-driven changes in tropical cyclone intensity shape dune activity on Earth’s largest sand island. *Geomorphology* 125 (1), 239–252.
- Levin, N., Ben-Dor, E., 2004. Monitoring sand dune stabilization along the coastal dunes of Ashdod-Nizanim, Israel, 1945–1999. *J. Arid Environ.* 58 (3), 335–355.
- Levin, N., Kidron, G.J., Ben-dor, E.Y.A.L., 2006. The spatial and temporal variability of sand erosion across a stabilizing coastal dune field. *Sedimentology* 53 (4), 697–715.
- Levin, N., Levental, S., Morag, H., 2012. The effect of wildfires on vegetation cover and dune activity in Australia’s desert dunes: A multisensor analysis. *Int. J. Wildland Fire* 21 (4), 459–475.
- Levin, N., Jablon, P.E., Phinn, S., Collins, K., 2017. Coastal dune activity and foredune formation on Moreton Island, Australia, 1944–2015. *Aeolian Res.* 25, 107–121.
- Li, Z., Guo, X., 2016. Remote sensing of terrestrial non-photosynthetic vegetation using hyperspectral, multispectral, SAR, and LiDAR data. *Prog. Phys. Geogr.* 40 (2), 276–304.
- Lyons, M.B., Keith, D.A., Phinn, S.R., Mason, T.J., Elith, J., 2018. A comparison of resampling methods for remote sensing classification and accuracy assessment. *Remote Sens. Environ.* 208, 145–153.
- Madurapperuma, B., Close, P., Fleming, S., Collin, M., Thuresson, K., Lamping, J., et al., 2018. Habitat mapping of Ma-le’l Dunes coupling with UAV and NAIP imagery. No. 7. In: *Multidisciplinary Digital Publishing Institute Proceedings*, p. 368.
- Marín, L., Forman, S.L., Valdez, A., Bunch, F., 2005. Twentieth century dune migration at the Great Sand Dunes National Park and Preserve, Colorado, relation to drought variability. *Geomorphology* 70 (1–2), 163–183.
- Mason, J.A., Swinehart, J.B., Lu, H., Miao, X., Cha, P., Zhou, Y., 2008. Limited change in dune mobility in response to a large decrease in wind power in semi-arid northern China since the 1970s. *Geomorphology* 102 (3–4), 351–363.
- Mather, P., Tso, B., 2016. *Classification Methods for Remotely Sensed Data*. CRC Press.
- Moulton, M.A., Hesp, P.A., Miot da Silva, G., Bouchez, C., Lavy, M., Fernandez, G.B., 2019. Changes in vegetation cover on the Youngusband Peninsula transgressive dunefields (Australia) 1949–2017. *Earth Surf. Proc. Land.* 44 (2), 459–470.

- Nield, J.M., Wiggs, G.F., Squirrell, R.S., 2011. Aeolian sand strip mobility and protodune development on a drying beach: examining surface moisture and surface roughness patterns measured by terrestrial laser scanning. *Earth Surf. Proc. Land.* 36 (4), 513–522.
- Nolet, C., van Puijenbroek, M., Suomalainen, J., Limpens, J., Rijsen, M., 2018. UAV-imaging to model growth response of marram grass to sand burial: implications for coastal dune development. *Aeolian Res.* 31, 50–61.
- Olofsson, P., Foody, G.M., Herold, M., Stehman, S.V., Woodcock, C.E., Wulder, M.A., 2014. Good practices for estimating area and assessing accuracy of land change. *Remote Sens. Environ.* 148, 42–57.
- Pickart, A.J., 2021. *Ammophila* invasion ecology and dune restoration on the West Coast of North America. *Diversity* 13 (12), 629.
- Provoost, S., Jones, M.L.M., Edmondson, S.E., 2011. Changes in landscape and vegetation of coastal dunes in northwest Europe: a review. *J. Coast. Conserv.* 15 (1), 207–226.
- Pye, K., Blott, S.J., Howe, M.A., 2014. Coastal dune stabilization in Wales and requirements for rejuvenation. *J. Coast. Conserv.* 18 (1), 27–54.
- Ryu, W., Sherman, D.J., 2014. Foredune texture: Landscape metrics and climate. *Ann. Assoc. Am. Geogr.* 104 (5), 903–921.
- Seifan, M., 2009. Long-term effects of anthropogenic activities on semi-arid sand dunes. *J. Arid Environ.* 73 (3), 332–337.
- Shumack, S., Hesse, P., Turner, L., 2017. The impact of fire on sand dune stability: Surface coverage and biomass recovery after fires on Western Australian coastal dune systems from 1988 to 2016. *Geomorphology* 299, 39–53.
- Smyth, T., Thorpe, E., Rooney, P., 2020. Blowout Evolution Between 1999 and 2015 in Ainsdale Sand Dunes National Nature Reserve, England. *North West Geogr.* 20 (1).
- Thomas, D.S., Leason, H.C., 2005. Dunefield activity response to climate variability in the southwest Kalahari. *Geomorphology* 64 (1–2), 117–132.
- Tsoar, H., Blumberg, D.G., 2002. Formation of parabolic dunes from Barchan and transverse dunes along Israel's Mediterranean coast. *Earth Surf. Proc. Land.* 27 (11), 1147–1161.
- van Boxel, J.H., Jungerius, P.D., Kieffer, N., Hampele, N., 1997. Ecological effects of reactivation of artificially stabilized blowouts in coastal dunes. *J. Coast. Conserv.* 3 (1), 57–62.
- Wolfe, S. A., Huntley, D. J., & Ollerhead, J., 1995. Recent and late Holocene sand dune activity in southwestern Saskatchewan. *Geological Survey of Canada, Ottawa, Current research 1995-B, 131-138.*
- Wolfe, S.A., Hugenholz, C.H., Evans, C.P., Huntley, D.J., Ollerhead, J., 2007. Potential aboriginal-occupation-induced dune activity, Elbow Sand Hills, northern Great Plains, Canada. *Great Plains Res.* 173–192.
- Zhen, Z., Quackenbush, L.J., Stehman, S.V., Zhang, L., 2013. Impact of training and validation sample selection on classification accuracy and accuracy assessment when using reference polygons in object-based classification. *Int. J. Remote Sens.* 34 (19), 6914–6930.